ISSN 1674-1056
http://cpb.iphy.ac.cn
http://iopscience.iop.org/cpb
中国物理 B
Chinese Physics
中国物理 Chinese Physics B

Structural, vibrational, optical, photoluminescence, thermal, dielectric, and mechanical studies on zinc (tris) thiourea sulfate single crystal:A noticeable effect of organic dye

Mohd Shkir, V Ganesh, S AlFaify, I S Yahia, Mohd Anis
Citation: Chin. Phys. B . 2018, 27(5): 054217. **doi:** 10.1088/1674-1056/27/5/054216

Journal homepage: http://cpb.iphy.ac.cn; http://iopscience.iop.org/cpb

What follows is a list of articles you may be interested in

Intensities and spectral features of the $^4I_{13/2}$-$^4I_{15/2}$ potential laser transition of Er^{3+} centers in CaF_2-CeF_3 disordered crystal

Qing-Guo Wang(王庆国), Liangbi Su(苏良碧), Jun-Fang Liu(刘军芳), Bin Liu(刘斌), Feng Wu(吴锋), Ping Luo(罗平), Heng-Yu Zhao(赵衡煜), Jiao-Jiao Shi(施佼佼), Yan-Yan Xue(薛艳艳), Xiao-Dong Xu(徐晓东), Witold Ryba-Romanowski, Piotr Solarz, Radoslaw Lisiecki, Zhan-Shan Wang(王占山), Hui-Li Tang(唐慧丽), Jun Xu(徐军)
Chin. Phys. B . 2017, 26(11): 114208. **doi:** 10.1088/1674-1056/26/11/114208

Diode-pumped laser performance of Tm:Sc_2SiO_5 crystal at 1971 nm

Bin Liu(刘斌), Li-He Zheng(郑丽和), Qing-Guo Wang(王庆国), Jun-Fang Liu(刘军芳), Liang-Bi Su(苏良碧), Hui-Li Tang(唐慧丽), Jie Liu(刘杰), Xiu-Wei Fan(范秀伟), Feng Wu(吴锋), Ping Luo(罗平), Heng-Yu Zhao(赵衡煜), Jiao-Jiao Shi(施佼佼), Nuo-Tian He(何诺天), Na Li(李纳), Qiu Li(李秋), Chao Guo(郭超), Xiao-Dong Xu(徐晓东), Zhan-Shan Wang(王占山), Jun Xu(徐军)
Chin. Phys. B . 2017, 26(8): 084203. **doi:** 10.1088/1674-1056/26/8/084203

Optical properties of Mg^{2+}, Yb^{3+}, and Ho^{3+} tri-doped $LiNbO_3$ crystals

Li Dai(代丽), Chun-Rui Liu(刘春蕊), Chao Tan(谭超), Zhe-Hua Yan(阎哲华), Yu-Heng Xu(徐玉恒)
Chin. Phys. B . 2017, 26(4): 044207. **doi:** 10.1088/1674-1056/26/4/044207

Carbon materials with quasi-graphene layers: the dielectric, percolation properties and the electronic transport mechanism

Lu Ming-Ming, Yuan Jie, Wen Bo, Liu Jia, Cao Wen-Qiang, Cao Mao-Sheng
Chin. Phys. B . 2013, 22(3): 037701. **doi:** 10.1088/1674-1056/22/3/037701

Improvement of dielectric tunability and loss tangent of (Ba,Sr)TiO_3 thin films with K doping

Zhang Wei-Jie, Dai Jian-Ming, Zhu Xue-Bin, Chang Qing, Liu Qiang-Chun, Sun Yu-Ping
Chin. Phys. B . 2012, 21(9): 097702. **doi:** 10.1088/1674-1056/21/9/097702

Experimental demonstration of narrow-band rugate minus filters using rapidly alternating deposition technology*

Ying Zhang(章瑛)[1], Yan-Zhi Wang(王胭脂)[2], Jiao-Ling Zhao(赵娇玲)[2], Jian-Da Shao(邵建达)[2], and Shuang-Chen Ruan(阮双琛)[1,†]

[1] *Shenzhen Key Laboratory of Laser Engineering, Key Laboratory of Advanced Optical Precision Manufacturing Technology of Guangdong Higher Education Institutes, College of Optoelectronic Engineering, Shenzhen University, Shenzhen* 518060, *China*

[2] *Key Laboratory of Materials for High Power Laser, Shanghai Institute of Optics and Fine Mechanics, Chinese Academy of Sciences, Shanghai* 201800, *China*

(Received 11 October 2017; revised manuscript received 18 February 2018; published online 26 April 2018)

The design, fabrication and performance of narrow-band rugate minus filters are investigated in this paper. A method of fabricating graded-index coatings by rapidly alternating deposition of low (SiO_2) and high (Al_2O_3) refractive index materials is presented to fabricate a rugate structure. The narrow-band rugate minus filter design and fabrication approaches are discussed in detail. The experimental results, including transmittance spectrum, surface damage test and damage morphology investigated with a scanning electron microscope, demonstrate the high performance of the as-fabricated spatial filter and confirm the feasibility of the fabrication method for narrow-band rugate minus filters.

Keywords: rugate structure, minus filter, narrow-band, laser-induced damage threshold (LIDT)

PACS: 42.79.Ci, 42.79.Wc **DOI:** 10.1088/1674-1056/27/5/054217

1. Introduction

Narrow-band minus filters are optical filters that selectively reject a wavelength band and transmit at both shorter and longer wavelengths.[1–5] They are widely used in laser radiation, Raman spectroscopy, etc. As an important kind of narrow-band minus filter, the rugate structure is a periodical thin film structure where the refractive index continuously varies with the film thickness,[6] e.g., as a sinusoidal function. Generally speaking, the rugate filter has the property that it can reflect a specific narrow-band spectrum and transmit all the other spectra. Compared with traditional filters, the Rugate filter can effectively prevent high-order reflection zones and has a better cut-off steepness, so it can theoretically control the locations and numbers of reflection zones and eliminate the stress interface of the film to obtain a higher laser-induced damage threshold (LIDT). It is particularly suitable for the weak spectral spectrum in a background with no bright spectrum, so it is used in the field of laser protection and others. Hence, it is widely regarded that the rugate filter has optical and mechanical properties that are different from those of discrete multilayer stacks, including efficient suppression of harmonics,[7] low stress,[8] higher scratch and wear resistance, superior laser-induced damage thresholds,[9] and higher temperature stability.[10]

Many efforts have been made to achieve high-performance rugate thin film filters by taking advantage of the unique properties of the rugate structure.[11–17] However, the preparation of the rugate filter is relatively difficult because of the requirement for accuracy in realizing the continuous refractive index profile. Several methods have been proposed and developed to fabricate the rugate filters, e.g., by mixing two or more materials with high and low refractive indices,[18–20] or by varying the content of the reactive gas with a single source.[21–23] However, further investigations are still required to testify the fabrication of narrow-band Rugate minus filters and analyze their application performances as spatial filters in high-power laser systems.

In this paper, we design and fabricate a narrow-band rugate minus filter. The rapidly alternating deposition technology, which employs pulsed direct current (DC) magnetron sputtering to fabricate Al_2O_3–SiO_2 composite films with Al and Si targets, is used to fabricate narrow-band Rugate minus filter sample. The experimental results show the measured transmittance spectra are in good agreement with the designed value. The laser-induced damage threshold (LIDT) of the narrow-band rugate minus filter is measured, and the damage morphology with scanning electron microscope (SEM) is observed, which confirms the potential of good performance of the internal adhesion of the film and the advantage of the gradient refractive index film.

2. Filter design

In this work, the spectral selectivity and angular spectral selectivity of the rugate filter are analyzed by the transfer matrix method, and the film is divided into finite uniform tandem structures. Like traditional multilayer dielectric films, the

*Project supported by the Postdoctoral Science Foundation of China (Grant Nos. 2016M592528 and 2016M602517), the Natural Science Foundation of Guangdong Province, China (Grant No. 2017A030310130), and the National Natural Science Foundation of China (Grant No. 11705259).

†Corresponding author. E-mail: scruan@szu.edu.cn

© 2018 Chinese Physical Society and IOP Publishing Ltd

rugate thin film structure is fabricated by using two materials with high and low refractive index. However, there is a fundamental difference between them. The multilayer dielectric film is formed by the vapor deposition of the two materials, while the rugate film is formed by materials whose refractive index is continuously changed. Therefore, for preparing the rugate film, the refractive index with gradient variation is realized by adjusting the ratio between the high refractive index material and the low one. Specifically, the automatic rate control of high and low refractive index materials should be carefully designed when using pulsed DC magnetron co-sputtering. The relative velocity is determined by the Drude model of the refractive index and the following equation:

$$n^2 = n_{\mathrm{L}}^2 X_{\mathrm{L}} + n_{\mathrm{H}}^2 X_{\mathrm{H}}, \tag{1}$$

where X_{H} and X_{L} represent the ratio between high and low refractive index materials, respectively; n_{H} and n_{L} denote the high and low refractive index of the two materials, respectively. In the coating process, through the high and low refractive index of the two materials using different evaporation rates, one can obtain a continuous change in refractive index and their evaporation rate R_{H} and R_{L} can be related by[18]

$$R_{\mathrm{L}} = \left(\frac{n_{\mathrm{H}}^2 - n^2}{n^2 - n_{\mathrm{L}}^2}\right) R_{\mathrm{H}}. \tag{2}$$

The advantage is that the two sources can be easily controlled and the gradient profile of refractive index change can be readily realized by continuously changing the deposition rate of one material or simultaneously changing the two evaporation sources.

To obtain a high reflectivity film in a limited wavelength range, the high and low refractive indexes alternate mutually and the thickness of each layer is a quarter wavelength. The width of the reflective band is related to the difference in refractive index between the materials constituting the multilayer film. The larger the difference in refractive index between the two films, the wider the reflection band is. The rugate minus filters also have the same properties. The combination of different materials can be coated with a different reflective bandwidth of the Rugate minus filter film. When the plating material is determined, the reflectivity of the film system is related to the number of cycles of the periodic elements of the film system. The more cycles, the higher the reflectivity of the film is. If the difference in refractive index between the two materials that constitute the Rugate minus filter is small and the number of cycles is large enough (i.e., thousands of cycles), the designed filter will have a narrow bandwidth and high reflectivity simultaneously. However, the difficulty of the experimental process will increase with the number of cycles, and the transmission characteristics will be more likely to be deteriorated. In this work, a preliminary experiment with 40 periods is carried out as a demonstration.

The narrow-band rugate minus filter possesses the refractive index profile of a continuous sinusoidal modulation as follows:

$$n(z) = n_{\mathrm{a}} + n_{\mathrm{p}} \sin(Kz + \Phi_0), \tag{3}$$

where n_{a} is the average refractive index and $n_{\mathrm{a}} = (n_{\mathrm{H}} + n_{\mathrm{L}})/2$, n_{p} is the difference between the high and low refractive index modulation of the film, Φ_0 is the initial phase of the film, K denotes the grating vector, the module of which is $2\pi/T$, T being the one-period thickness of the film. A 40-period rugate filter, which has a sinusoidal variation in the refractive index, is designed in this work.

Table 1. Simulation parameters for a narrow-band rugate minus filter film.

Parameter	Value	Parameter	Value
T	341.9 nm	N	40
λ_0	1053 nm	n_{p}	0.08
n_{H}	1.62	n_{a}	1.54
n_{L}	1.46		

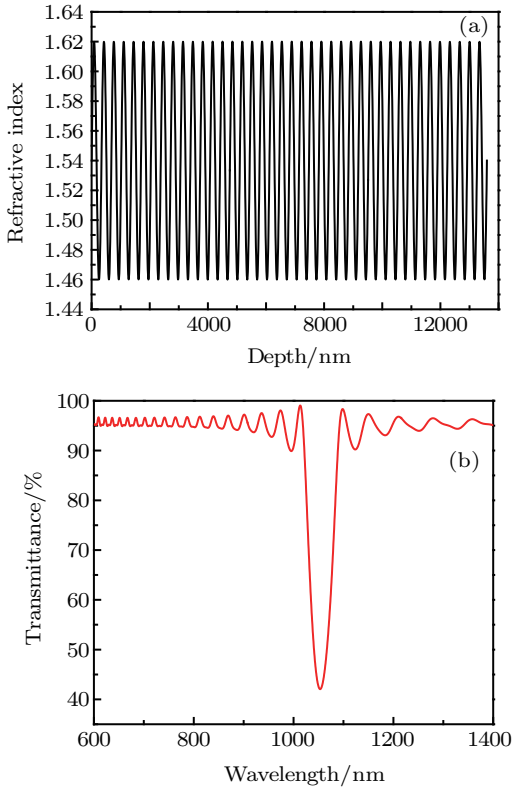


Fig. 1. (color online) (a) Schematic diagram of the refractive-index profile rugate structure and (b) corresponding calculated transmittance spectrum.

The values of n_{a} and n_{p} will influence the cut-off width of the transmission spectrum of the filter: the cut-off width of the transmission spectrum is proportional to the value of n_{p}, while inversely proportional to the value of n_{a}. The optical thickness

z will affect the cut-off depth of the transmission spectrum: the depth of the cut-off zone of the transmission spectrum is proportional to the value of optical thickness. In this work, air is selected as an incident medium, BK7 glass substrate is chosen as the outgoing medium and the sinusoidal rugate filter is designed accordingly. According to this principle, the transmission spectrum of narrow-band rugate minus filter is simulated by MatLab. Table 1 gives the values of the simulation parameters. The refractive index profile of the narrow-band rugate filter and the corresponding calculated transmittance spectra are shown in Fig. 1.

3. Experimental procedure

The narrow-band rugate filter was fabricated by combining rapidly alternating deposition technology. The method of fabricating the composite thin films by using pulsed direct-current magnetron sputtering with rapidly alternating deposition is presented and a diagram of the deposition chamber is shown in Fig. 2, where a computer is used to control the rapid rotation of the substrate.

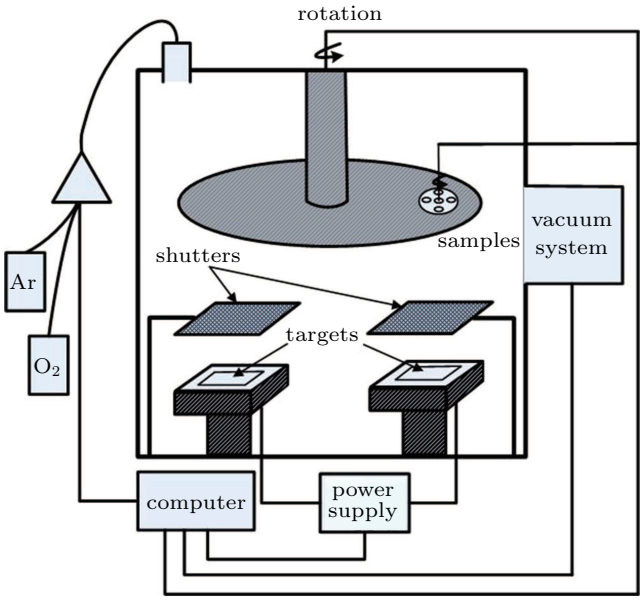


Fig. 2. (color online) Schematic diagram of a rapidly alternating deposition system.

The BK7 glass (φ30 mm×3 mm) substrates were ultrasonically cleaned in acetone and ethanol before being used in the vacuum system. The transmission spectra of the samples were measured by using a Lambda 1050 spectrophotometer (from 700 nm to 1500 nm). The cross-sectional microstructure was characterized by field emission scanning electron microscopy (Zeiss Auriga Crossbeam microscope). Laser damage experiments were carried out by using an optical pulse source with 12 ns duration from a 1053 nm Nd:YAG laser at an incidence angle of 0°.

The pulsed DC magnetron sputtering system was used in this experiment. Al (99.95% purity) and Si (99.999% purity) targets were used. The background pressure was 2.0×10^{-3} Pa before deposition and the sputtering pressure was kept at 0.5 Pa and the temperature was maintained at 120 °C in the sputtering process. Argon and oxygen were admitted to the process chamber with flow rates of 20 sccm and 30 sccm, respectively. The composite $(Al_2O_3)_{1-x}(SiO_2)_x$ thin films were fabricated by changing their powers. The power of Al target (P_{Al}) was varied in a range from 800 W to 1200 W and the powers of Si target (P_{Si}) change from 600 W to 200 W in steps of 1 W. The two values satisfy the following equation:

$$P_{Al} = 1000 + 200\sin(\pi t/180), \tag{4}$$

$$P_{Si} = 400 - 200\sin(\pi t/180). \tag{5}$$

4. Results and discussion

The measured transmittance spectra of the fabricated rugate narrow band minus filter and the corresponding calculation curve are given in Fig. 3. The dashed line is the measured rugate transmission spectrum curve that is recorded by the Lambda 1050. The measured full width at half maximum (FWHM) of the stopband is approximately 30 nm. It can be seen from the figure that the experimental and designed spectra are consistent with each other. It should be noted that the experimental result has a narrower bandwidth than the designed value. This could be due to inadequate control of refractive index in the reaction process. It is inferred that the difference in refractive index modulation between the two materials is smaller than the design value. The transmittance of the experiment is shallower than the design value, which is also attributed to the same reason that leads to a narrower bandwidth. The ripples on both sides of the stop band are caused by two factors: one is the difference in refractive index between the two materials of the filter; the other is that the rugate structure does not match the refractive indexes of the base and air.

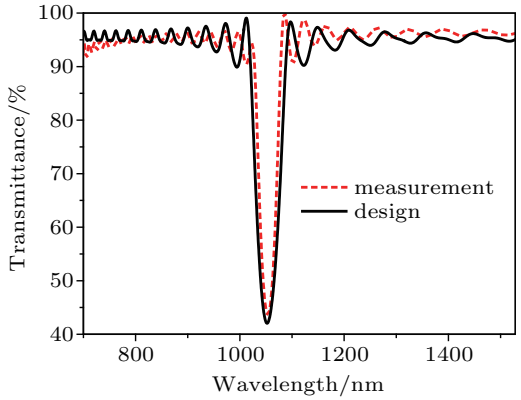


Fig. 3. (color online) Calculated and measured transmittance spectra of rugate narrow-band minus filter.

In order to study the relationship between the properties and the damage of the film, the surface of the film is tested by using our surface damage test platform. The measurement

mode is 1-on-1. After the damage test, figure 4 shows the rugate minus filter damage probability curve with a threshold of 3.3 J/cm^2 (12 ns).

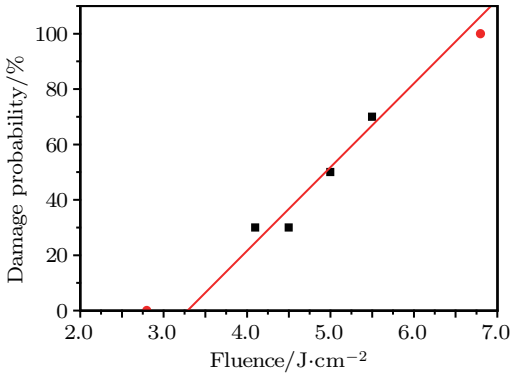


Fig. 4. (color online) Laser-induced damage threshold (LIDT) of the narrow-band rugate minus filter.

Figure 5 shows the combination of the refractive index profile and the electric field of the rugate minus filter. It is clear from the figure that the electric field distribution in the rugate film is mainly distributed on the surface of the film. Then we observe the damage morphology with the SEM. From the damage morphology, the laser-induced damage basically occurs at the substrate and the reasons could be due to defects caused by the coupling effect between the substrate and the film layer as shown in Fig. 6(a). Figure 6(b) shows that the change in the color of the film from the air to the substrate represents a change in the ratio between the two components in the mixed medium. The bright color represents the proportion of the Al_2O_3 component in the mixture. The higher the proportion, the greater the refractive index of the mixed medium is. It can be seen from the figure that the prepared film has no obvious interface and the gradual change of the color corresponds to the continuous change of the refractive index of the film. Therefore, the internal adhesion of the film is good and the advantage of the gradient refractive index film is further verified.

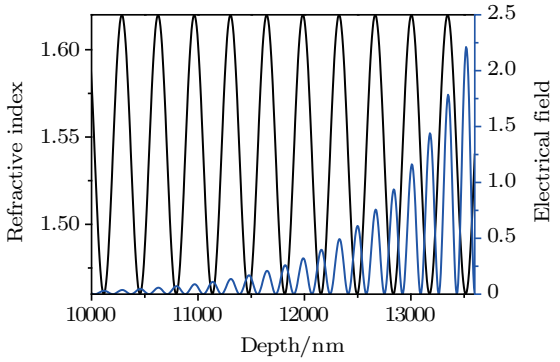


Fig. 5. (color online) Electric field distribution of the rugate minus filter.

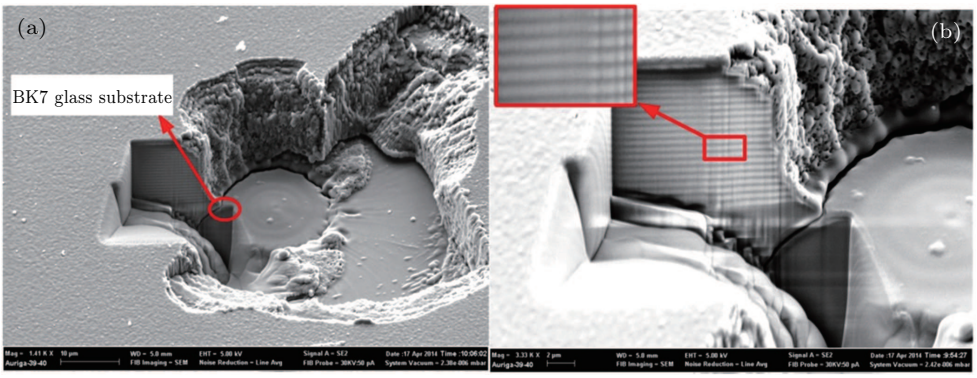


Fig. 6. (color online) Cross-sectional SEM micrograph of the sample.

5. Discussion

Narrow-band rugate minus filters are a promising solution to high-performance spatial filters in high power laser systems. In this work, we present the experimental demonstration of such a kind of spatial filter by using rapidly alternating deposition technology. However, it should be noted that some issues of the narrow-band rugate minus filters for low-pass filter devices need to be further investigated.

(i) The thicker film leads to longer preparation periods and thus a random error and a systematic error are easily brought in during the preparation process.

(ii) Since the angular bandwidth of the rugate minus filter is proportional to the difference in refractive index, it is necessary to have a smaller refractive index difference to pursue a narrower angular spectral selective bandwidth. However, it is difficult to find a suitable material to prepare a narrow-band rugate minus filter due to so few materials having smaller refractive index differences. Therefore, although the theoretical design of the narrow-band rugate minus filter can be achieved, there are still some challenges in their realization.

6. Conclusions

Narrow-band rugate minus filters are prepared experimentally by using rapidly alternating deposition technology in this work. The measured transmittance spectra of the fabricated samples are in excellent agreement with the theoretical

calculations. The samples have the potential of good performance of rather smooth interfaces, internal adhesion of the film and the advantage of the gradient refractive index film, which are confirmed by LIDT test and SEM observation. Although as a preliminary demonstration in this work, the results indicate that it is an effective approach to using rapidly alternating deposition technology to realize high-performance narrow-band rugate minus filters. Therefore, the narrow-band rugate minus filters can find important applications in high-power laser systems since their whole systems can be greatly simplified. Future work will focus on refining the experimental process and optimizing the selection of materials.

References

[1] Hawkeye M M and Bertt M J 2006 *J. Appl. Phys.* **100** 044322
[2] Leitel R, Stenzel O, Wilbrandt S, Gäbler D, Janicki V and Kaiser N 2006 *Thin Solid Films* **497** 135
[3] Zhang Y, Qi H J, Yi K, Wang Y Z, Sui Z and Shao J D 2015 *Chin. Phys. B* **24** 054212
[4] Zhang Y, Qi H J, Yi K, Wang Y Z, Sui Z and Shao J D 2015 *Chin. Phys. B* **24** 0104216
[5] Liu J T, Zhou Y S, Wang F H and Gu B Y 2005 *Chin. Phys.* **14** 2474
[6] Bovard B G 1993 *Appl. Opt.* **32** 5427
[7] Baumeister P W 1985 *Appl. Opt.* **24** 2687
[8] Tang C J, Jaing C C, Lee K S and Lee C C 2008 *Appl. Opt.* **47** C167
[9] Jupe M, Lappschies M, Jensen L, Starke K and Ristau D 2007 *Proccedings of SPIE* Vol. 6403 64031A-1
[10] Polenzky C, Rickers C and Vergöhl M 2009 *Thin Solid Films* **517** 3126
[11] Johnson W E and Crane R L 1993 *Proceeding of SPIE 2046 on Inhomogeneous and Quasi-Inhomogeneous Optical Coatings* 88
[12] Southwell W H, Hall R L and Gunning W J 1993 *Proceeding of SPIE 2046 on Inhomogeneous and Quasi-Inhomogeneous Optical Coatings* 46
[13] Southwell W H 1997 *Appl. Opt.* **36** 314
[14] Zhang J C, Fang M and Shao Y C 2012 *Chin. Phys. B* **21** 054219
[15] Zhang J C, Fang M and Shao Y C 2011 *Chin. Phys. B* **20** 094212
[16] Allen J and Herrington B 1993 *Proceeding of SPIE 2046 on Inhomogeneous and Quasi-Inhomogeneous Optical Coatings* 126
[17] Zheng G W 2011 (Ph. D. Dissertation) (Changsha: National University of Defense Technology
[18] Gunning W J, Hall R L, Woodberry F J, Southwell W H and Gluck N S 1989 *Appl. Opt.* **28** 2945
[19] Lee C C, Tang C J and Wu J Y 2006 *Appl. Opt.* **45** 1333
[20] Liu L and Su X R 2008 *Chin. Phys. B* **17** 2170
[21] Bartzsch H, Lange S, Frach P and Goedicke K 2004 *Surf. Coat. Tecnol.* **180–181** 616
[22] Katagiri Y and Ukita H 1990 *Appl. Opt.* **29** 5074
[23] Shen Z C, Shao J D, Wang Y J and Fan Z X 2005 *Acta Phys. Sin.* **54** 4842 (in Chinese)